DOI: 10.1007/s12541-010-0041-0

Micro Grooving Simulation and Optimization in the Roughing Stage

Jong-Min Lee[1], Tae-Jin Je[2], Doo-Sun Choi[2], Seok-Woo Lee[3], Duy Le[1] and Su-Jin Kim[1,#]

1 School of Mechanical and Aerospace Engineering, Gyeongsang National University, 900, Gajwa-dong, Jinju-si, Gyeongnam, South Korea, 660-701
2 Korea Institute of Machinery & Materials, 104, Sinseongno, Yuseong-gu, Daejeon, South Korea, 305-343
3 Korea Institute of Industrial Technology, 35-3, Hongcheon-ri, Cheonan-si, Chungnam, South Korea, 331-825
Corresponding Author / E-mail: sujinkim@gnu.ac.kr, TEL: +82-55-751-6075, FAX: +82-55-762-0227

KEYWORDS: Manufacturing Simulation, Micro Pattern, Specific Cutting Energy, Micro Grooving, Reduce Roughing Time

The micro pattern machining on the surface of a wide mold is not easily simulated and optimized using conventional methods. This paper represents the micro pattern cutting simulation software. The software simulates micro pattern grooving in 3D geometry, predicts the cutting force and optimizes the time factor in the roughing stage. The v-groove for prism and pyramid patterns and the rectangular groove for rectangular and pillar patterns are simulated. The code of this program is built using visual C++ and OpenGL.

Manuscript received: March 11, 2009 / Accepted: January 20, 2010

NOMENCLATURE

F_c = cutting force
K = specific cutting energy
A = cutting area
C = experimental constant
n = experimental constant
t = chip thickness
d_i = cutting depth at i^{th} step
a = angle of diamond tool and pattern
p = pitch between each pattern
w = width of rectangular tool and pattern
F_n = the maximum permissible cutting force
d_{pi} = depth of pyramid pattern
d_{ri} = depth of pillar pattern
d_n = final cutting depth
δd_i = relative cutting depth
F_i = i_{th} cutting force
F_{avg} = average cutting force
δd_{avg} = relative cutting depth's average
m = number of cutting cycle

1. Introduction

The light guide panel of a liquid crystal display or the deflection sheet of traffic signs is a wide sheet including a large number of micro patterns that are designed to refract or reflect light. The huge amount of micro patterns on the wide sheet is produced using a roll mold or plate mold. The molds are machined by micro grooving using a single crystal diamond tool.[1]

In order to stay competitive in today's international markets, companies must deliver new, high-quality products in a short time with a variety of versions at minimum cost. Manufacturing simulation is rapidly rising in today's international markets as an interesting strategy for product development. Its primary aim was reducing the lead time to market and costs associated with new product development. Manufacturing simulation offers a test platform for the time-consuming and expensive physical experiments. Micro machining in particular has challenges and limitations, because simple scaling cannot be applied to modeling the phenomena of micro processing.

The machining simulation was studied for milling and the precise turning process.[2-4] The study continued to the experimental and analytical research of the micro cutting process.[5-8] Unlike conventional macro-machining processes, micro-machining displays different characteristics due to its significant size reduction. Most chip formation investigations are derived from macro-ultra-precision diamond and hardened steel cutting operations; numerous publications have focused on the effect of round edges and minimum chip thickness.[5] Often, the edge radius of the tools is relatively larger than the chip thickness. In contrast to the conventional sharp-edge cutting model, chip shear in micro-

machining occurs along the rounded tool edge.[8] As a result, cutting has a large negative rake angle, which affects the magnitude of the plowing and shearing forces. Therefore, a relatively large volume of material has to become fully plastic for a relatively small amount of material to be removed, resulting in significant increases in specific energy levels.[6,7] Further, when the chip thickness is below a critical point, chips may not be generated during the cutting process; instead, the workpiece material elastically deforms. Critical chip thickness is proposed to be a quarter of the size of cutter edge radius.[6]

The edge radius of the diamond tool used in this research is less than 0.1 μ m and the chip thickness in the roughing stage is much bigger than 0.025 μ m. Thus, the cutting force model does not consider plowing effects and elastic recovery but takes into account a significant increase in specific cutting energy that occurs when chip thickness is decreased.

The finite element method was also used to predict the cutting process.[9,10] The nano-scale machining simulation is now possible using the molecular dynamics approach and finite element method.[11-13]

Current research for the micro pattern grooving simulation and cycle time optimization of the surface of wide molds is insufficient. The micro grooving force prediction model specialized for prism, rectangular, pyramid and pillar patterns needs to be developed. The micro grooving condition used to optimize the time factor needs to be suggested to ensure an effective tool path output after simulation. Software needs to be developed to apply the suggested prediction and optimization algorithm automatically.

In this paper, several key issues for developing a micro grooving optimization platform using virtual manufacturing technology are discussed, i.e., representation of micro cutting force modeling, introducing a method of predicting cutting force, simulating the grooving process and proposing optimized cutting conditions. All issues are built upon one program. Its functions are predicting cutting force, simulating a grooving process in 3D space and controlling cutting depth to optimize the time factor. The v-groove for prism and pyramid patterns and the rectangular groove for rectangle and pillar patterns are simulated. Here, we only consider the roughing stage because in finishing, the stage quality factor is more important than the time factor.

2. Cutting Force Analysis

2.1 Cutting force model

The principles of micro-machining are similar to conventional cutting operations. The surface of the workpiece is mechanically removed using micro-tools. The cutting force is directly related to chip formation. It is suitable to develop a micro cutting force model according to the specific cutting energy.

Considering the physical conditions that occur in the micro-domain, a cutting force analyzing technique will be applicable to micro cutting development. The developing program predicts the cutting force of micro grooving with the experimental constant, which is calculated from the experimental results. Due to specific cutting energy, the cutting force is calculated generally in the cutting cross section.

$$F_c = KA, \text{ where } K = Ct^{-n} \tag{1}$$

The cutting force model of prism patterns is shown in equation (2) when the cutting width is smaller than the pitch. This usually happens at the roughing step, as shown in Fig. 1(a). The finishing force model is shown in equation (3) when the width is bigger than the pitch and the prism pattern is formed.

$$F_c = C\left((d_i - d_{i-1})\sin\left(\frac{a}{2}\right)\right)^{-n}\left(d_i^{\,2} - d_{i-1}^{\,2}\right)\tan\left(\frac{a}{2}\right) \tag{2}$$

$$F_c = C\left((d_i - d_{i-1})\sin\left(\frac{a}{2}\right)\right)^{-n}(d_i - d_{i-1})\,p \tag{3}$$

For rectangular patterns, the cutting area is divided into the bottom and two side sections and the corner regions are considered bottom section as shown in Fig. 1(b). The cutting forces of the bottom and two side sections are computed as shown in equation (4).

$$\begin{aligned} F_c = {} & C\left((d_i - d_{i-1})\sin\left(\frac{a}{2}\right)\right)^{-n} 2d_{i-1}(d_i - d_{i-1})\tan\left(\frac{a}{2}\right) \\ & + C(d_i - d_{i-1})^{-n}\left(w + (d_i - d_{i-1})\tan\left(\frac{a}{2}\right)\right)(d_i - d_{i-1}) \end{aligned} \tag{4}$$

The experimental constant C and n are determined for the purpose of minimizing the error of the measurement cutting force F_{real} and the prediction cutting force F_{mod} following the least square method.

$$\min[\sum(F_{\text{mod}} - F_{real})^2] \rightarrow C, n \tag{5}$$

The pyramid pattern is fabricated by cutting a prism pattern along the perpendicular direction with the same tool and pitch. The first cutting direction is exactly the same as the prism pattern; the second cutting direction is different because the starting plate already includes a prism pattern perpendicular to the cutting direction, as shown in Fig. 1(c). The depth wave function of the pyramid pattern is suggested in equation (6), and the cutting force is computed by inserting cutting depth d_{pi} into the equation (2). Fig. 1(e) shows the cutting force when the pyramid pattern is grooved on the prism pattern plate.

$$\begin{aligned} & d_{pi}(x) = 0 && if && 0 \le x < (d_n - d_i)\tan(a/2) \\ & d_{pi}(x) = \frac{x}{\tan(a/2)} + d_i - d_n && if && (d_n - d_i)\tan\left(\frac{a}{2}\right) \le x < \frac{p}{2} \\ & d_{pi}(-x + p) = d_{pi}(x) \quad d_{pi}(x + pm) = d_{pi}(x) && (mirror \,\&\, array) \end{aligned} \tag{6}$$

The pillar pattern is fabricated by cutting a rectangular pattern along the perpendicular direction with the same tool and pitch. The second direction cutting plate includes a rectangular pattern perpendicular to the cutting direction, as shown in Fig. 1(d). The depth wave function of the pillar pattern is suggested in equation (7), and the cutting force is computed by inserting cutting depth d_{ri} into the equation (4).

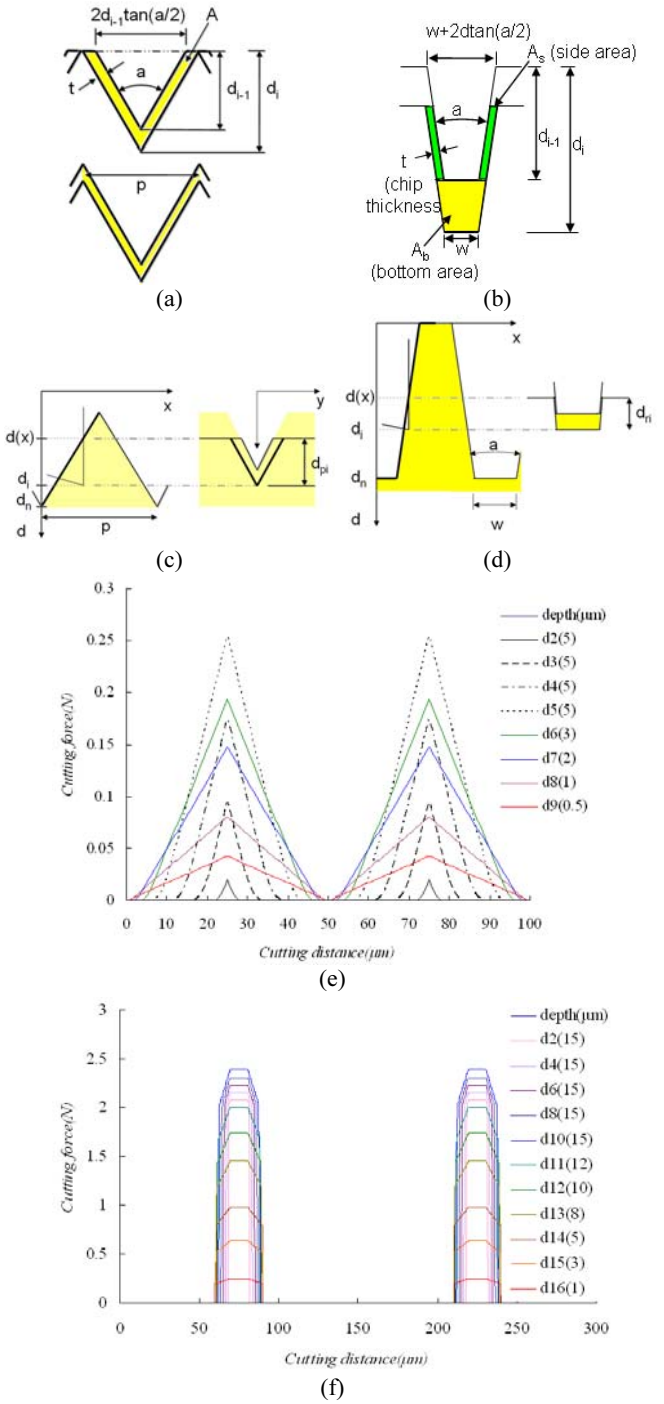

Fig. 1 (a) (b) Cutting area of prism and rectangular patterns (c) (d) Cutting depth of pyramid and pillar patterns (e) Cutting force of pyramid pattern (f) Cutting force of pillar pattern

Fig. 1(f) shows the cutting force when the pillar pattern is grooved on the rectangular pattern plate. The pitch is 150 μm, the angle is 5.72° and the width is 120 μm.

$$
\begin{aligned}
&d_{ri}(x)=0 && if \quad 0\le x<w/2+(d_n-d_i)\tan(a/2)\\
&d_{ri}(x)=\frac{x-w/2}{\tan(a/2)}+d_i-d_n && if \quad \frac{w}{2}+(d_n-d_i)\tan\left(\frac{a}{2}\right)\le x<\frac{w}{2}+d_n\tan\left(\frac{a}{2}\right)\\
&d_{ri}(x)=d_i && if \quad \frac{w}{2}+d_n tai\left(\frac{a}{2}\right)\le x<p/2\\
&d_{ri}(-x+p)=d_{ri}(x) \quad d_{ri}(x+pm)=d_{ri}(x) && (mirror\ \&\ array)
\end{aligned}
\tag{7}
$$

2.2 Comparison of model with experimental data

2.2.1 Experiment equipments

The experiment for this study was conducted using the equipment at the Korea Institute of Machinery and Materials. The configuration of the precise machine tool, workpiece and single crystal diamond tool is shown in Fig. 2. The specification of the precise machine tool is at Table 1. Alongside the primary X, Y and Z axes, a turning axis was added. The X and Y axes were implemented with an air bearing structure with a maximum position error of 20 nm and average velocity error of 2%. The Z axis did not have any back lash, and a counter balance device was placed on the side of the lead screw to withstand high loads. The PC-based motion controller used the PMAC1 board from Deltatau, which is capable of controlling eight axes. A Kistler Co. 9256A2 3-axis dynamometer was attached to the bottom of the workpiece to measure the cutting forces and the specification of the cutting force measurement system is in Table 2.

Machine tools Tool and stock

Fig. 2 Experimental equipment

Table 1 Specification of the cutting machine

Item		Unit	Specifications
Table	Size	mm	220×220
	Allowable weight	N	890
X-Y Axis Stage	Moving Stroke	mm	200×200
	Min. Incremental Move	nm	5 (200,000cts/mm)
Z Axis Slide	Moving Stroke	mm	100 (LS1mm/rev)
	Min. Incremental Move	nm	40 (25,000cts/mm)

Table 2 Specification of the cutting force measurement system

Dynamometer	Kistler Co., 9256A2
Amplifier	Kistler Co., 5019B130
Data Acquisition System	NI 6012E DAQCard-Al-16XE-50

The workpiece is 6:4 brass that was used for micro pattern plate mold in industries. The cutting speed was 1200 mm/min and cutting depth was different at each experiment.

2.2.2 Prism pattern

A v-shaped single crystal diamond tool with 90° angle was used to fabricate a prism pattern with 50 μm pitch. The SEM images of prism patterns at each cutting step are shown in Fig. 3(a). The cutting forces were measured during the experiment to build and verify the cutting force model of this paper.

The cutting force model of a prism pattern was developed using the cutting mechanism in equation (1) and experimental data in Fig.

3(a). The experimental constant C and n were computed using the least square method. The graph of the developed model and the measure data are plotted together. The cutting direction is shown on the y axis and the vertical direction is shown on the z axis in the graph.

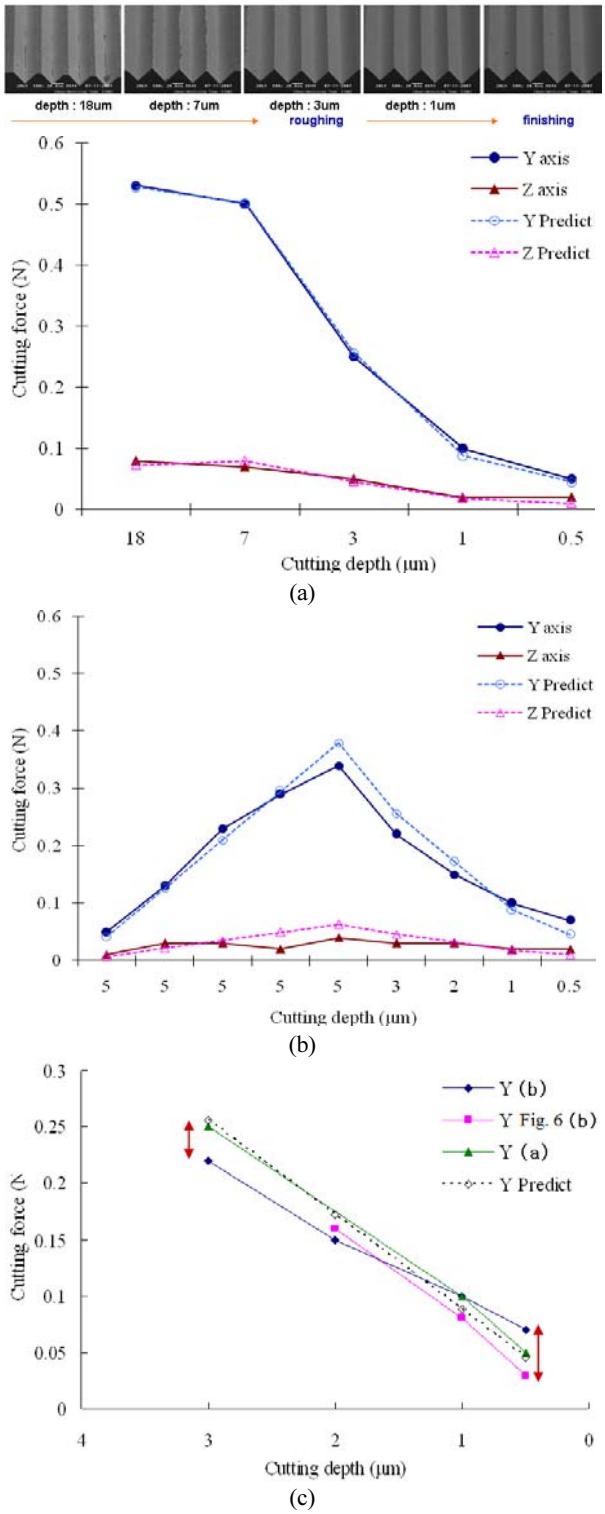

Fig. 3 (a) Force model developed from experimental data of the prism pattern: C_y=0.00174, n_y=0.026, C_z=0.00035, n_z=0.172 (b) Force predicted by model (a) and measured force: Maximum error is 0.04 N (c) Measured error of each experiment: Maximum measured error is 0.04 N

The cutting force model, developed by the first experiment, was verified by the following experiment. The cutting force predicted by the developed model was compared to another experimental data set. The maximum error between the predicted and measured cutting forces is 0.04 N in the second experiment, as shown in Fig. 3(b). There were errors among the three experiments. The cutting forces at the common cutting depths are plotted in Fig. 3(c). The maximum error between the experimental data was 0.04 N, which shows that the error in the developed model is derived from the model itself and the noise of the measured data. It was proved that the micro pattern cutting force prediction model works well on prism patterns, because the errors between the cutting force predicted by the model developed in the first set of experimental data and the measured cutting force in the second and third experiments were smaller than 0.04 N.

2.2.3 Rectangular pattern

A rectangular-shaped diamond tool with 120 μm width and 5.72° taper angle was used to fabricate a rectangular pattern. The SEM images of rectangular patterns at each cutting step are shown

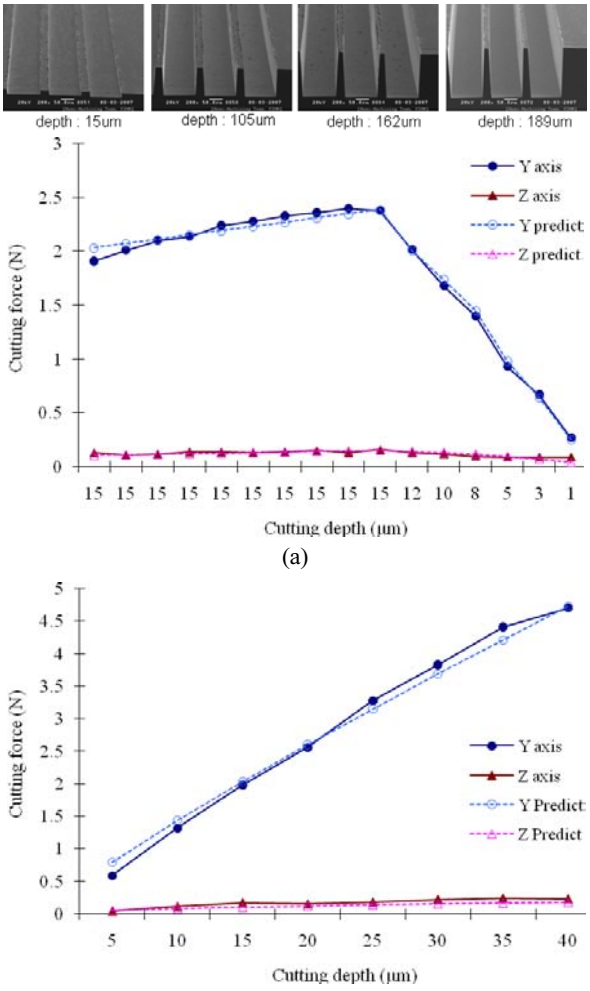

Fig. 4 (a) Force model developed from experimental data of the rectangular pattern: C_y=0.00168, n_y=0.149, C_z=0.00021, n_z=0.468 (b) Force predicted by model (a) and measured force: Maximum error is 0.21 N

in Fig. 4(a). The cutting forces were measured during the experiment to build and verify the cutting force model of this paper.

The cutting force model of the rectangular pattern was developed using equation (4) and the experimental data in Fig. 4(a). The model was made using both theory and data from the first experiment. The cutting forces of the model and the experimental data were plotted together.

The cutting force predicted by the developed model was compared to data from the second experiment. The maximum error between the predicted and measured cutting forces is 0.21 N in the second experiment, as shown in Fig. 4(b). It was proved that the micro pattern cutting force prediction model works well for rectangular patterns, because the error between the cutting force predicted by the model and the measured cutting force was small.

3. Micro Pattern Cutting Simulation

3.1 Automatic Computation of the Cutting Section

The cutting section needs to be computed to predict the micro cutting force and suggest optimal cutting depths automatically. The 3D geometrical micro cutting simulation software is developed to compute the cutting section used to predict grooving mechanism and optimize cutting conditions automatically.

The flowchart of the developed micro pattern cutting simulation software is shown in Fig. 5(a). The geometrical cutting simulation computes the remaining geometry and cutting section. The micro cutting force is computed automatically with the micro cutting force model, and the cutting section is computed using geometrical grooving simulation. Finally, the optimal cutting depths that make the cutting forces uniform are used as output for effective tool path generation. The developed program will be able to increase the productivity of the micro pattern grooving on a wide mold by applying the suggested conditions.

3.2 3D Visualization of the Micro Pattern

It will take too long to visualize several million patterns on a single display. This research reduced the rendering time by arraying a basic pattern in the zoomed window of display. The pattern shapes are expressed by the boundary representation method, which is more precise than sampled representation.

The data structure of the software shown in Fig. 5(b) is designed to be useable for various sections and multiple grooving directions. The software simulates prism, rectangular, pyramid, pillar, half circle prisms and various angle prisms, as shown in Fig. 5(c). The random pattern is fabricated using a fast tool servo vibrating micro tool. The software simulates a micro pattern curved randomly, as shown in Fig. 5(d). The grooving process visualization is useful because the real cutting process is difficult for the user to see due to critical temperature control of the environment and small pattern size.

3.3 Micro Cutting Simulator

The purpose of the developed micro pattern cutting simulation program is automation in micro grooving. It will be very convenient

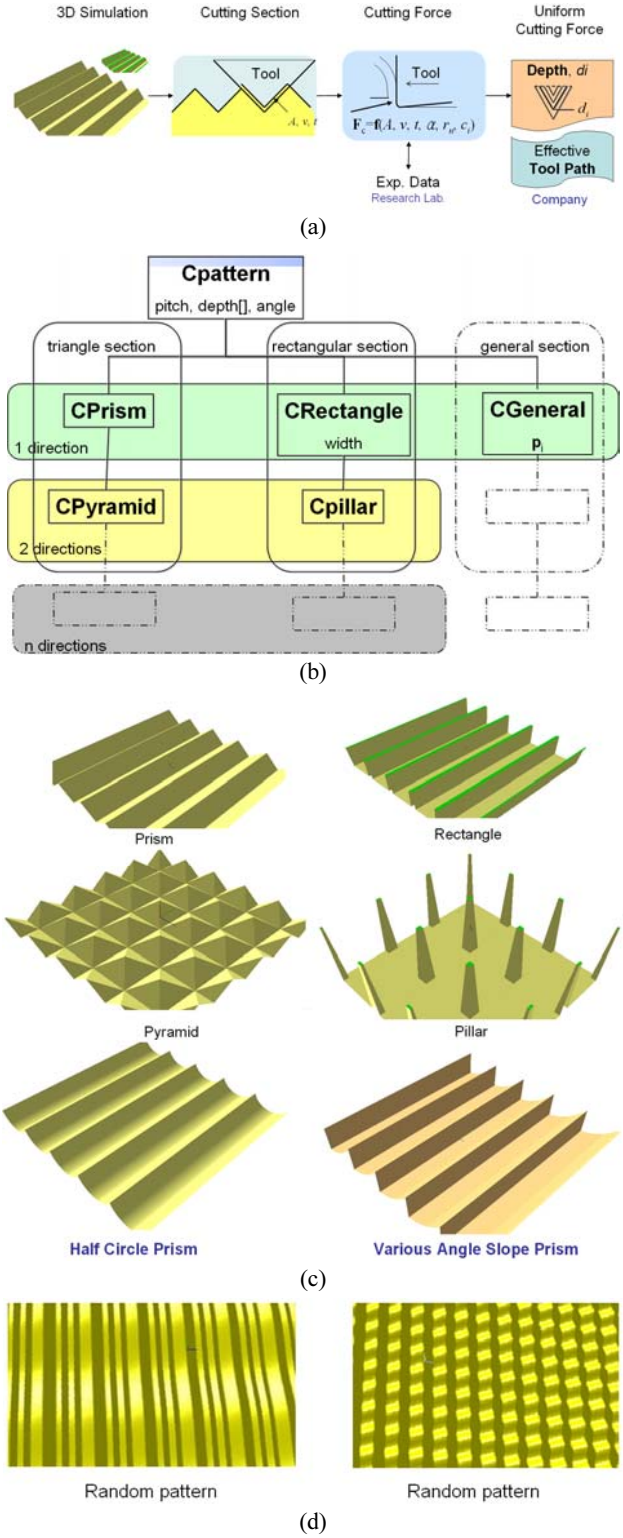

Fig. 5 (a) Flow chart of micro cutting simulation software (b) Data structure of the micro pattern geometry (c) Visualization of micro cutting simulation results (d) Visualization of random pattern cut by fast tool servo

for the users, since they will simply need to enter the necessary information for machining, such as groove type and pattern size, at the graphic user interface. The software simulates the groove forming process onscreen and produces cutting depth automatically to optimize the time factor.

4. Optimize Cutting Time

4.1 Cutting Depth for Time Factor

It takes a long time to groove a huge amount of micro patterns on the wide roll mold or plate mold using a single crystal diamond tool. The primary aim of simulation is reducing the lead time to market.

Since the ultimate objective of this study is to expedite processing, we focused on reducing the number of processing cycles in the roughing stage. Traditionally, roughing of a metal plate involved multiple processing cycles at a specified uniform depth. For example, roughing of 25 μm required five cycles of 5 μm processing. Processing 25 μm with five cycles of 5 μm processing on a flat mold of a size of 200 x 200 mm requires over 55 hours, which means it takes 11 hours for a single roughing cycle. Our goal is to reduce the number of cycles and thereby the total processing time by varying the processing depth for each cycle.

Uniformly increasing the processing depth to reduce the number of cycles is likely to force the processing to exceed the maximum cutting force, causing damage to the tools. Therefore, the objective of this study is to maintain the cutting force within the permissible range and reducing the number of cycles while making sure that no damage is inflicted on the tools. This paper suggested a new method that reduces the cycle time of the roughing stage.

The optimization variables are cutting depths d_i and the goals are to minimize the number of cutting cycle m and to make uniform the cutting forces F_i. The boundary conditions are total cutting depth d_n and the maximum permissible cutting force F_n which should be bigger than the uniformed cutting forces.

4.2 Algorithm and Flow Chart

The constant cutting depths at the roughing stage increased the cutting force from 0.05 N to 0.35 N, as shown in Fig. 3(b). This paper proposed a new algorithm that produces variable cutting depths to standardize the cutting force and reduce roughing time. Unlike the conventional roughing process, the proposed algorithm varies the processing depth for each cycle based on the prediction equations in order to maximize the cutting depth while maintaining the cutting force at a uniform level. The algorithm proposed in this paper was constructed with equations derived from the experimental constants found from previous experiments to predict the cutting force applied to the tools.

The procedure that produces cutting depths on the condition of a standardized cutting force is shown in the flowchart of Fig. 6(a). The input of this module is total roughing depth d_n and the maximum permissible cutting force F_n.

The algorithm consists of three sections. First, the total roughing depth is divided by the number of processing cycles m to predict the cutting force F_i at each cutting depth. The cutting force of each step is computed using the model developed in the previous chapter.

Second, the maximum and minimum cutting forces at each predicted depth are compared to determine whether they are within the permissible range at small loop. Each cutting depth is compensated for by the ratio of cutting force and average cutting force, as shown in equation (8).

$$\delta d_i += \left(1 - \frac{F_i}{F_{avg}}\right)\delta d_{avg}, \text{ where } \delta d_i = d_i - d_{i-1} \tag{8}$$

The small loop will end when the differences between the cutting forces are smaller than 0.001 N.

Third, if the uniformed cutting force F_{max} is bigger than the maximum permissible cutting force F_n, the number of processing cycles m is increased and return to the first step. The big loop will end when the uniformed cutting force is smaller than the maximum permissible cutting force.

Through this flow chart, the adjusted cutting depths d_i are generated along with the uniformed cutting forces F_i and the reduced number of cutting cycles m.

4.3 Cycle Time Reduction Result

In the roughing stage with a standardized cutting depth, the cutting force increased rapidly, as shown in Fig. 3(b). The cutting force reaches 0.35 N at the fifth depth, which was seven times larger than the 0.05 N force at the first depth. By applying the new algorithm, the cutting force is standardized to 0.35 N when the cutting depths are changed to 14.6, 5.9 and 4.5 μ m, as shown in Fig. 6(b).

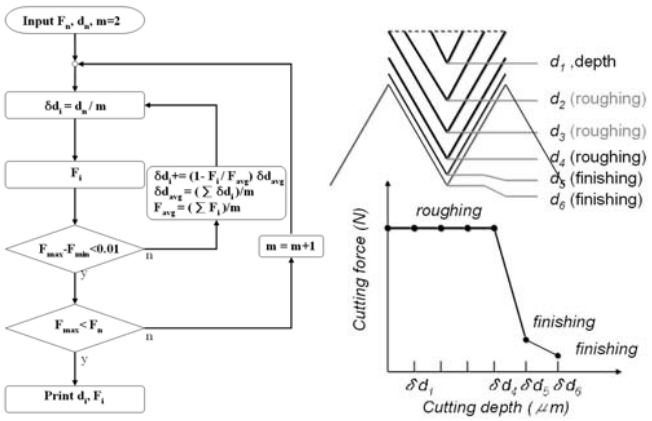

(a)

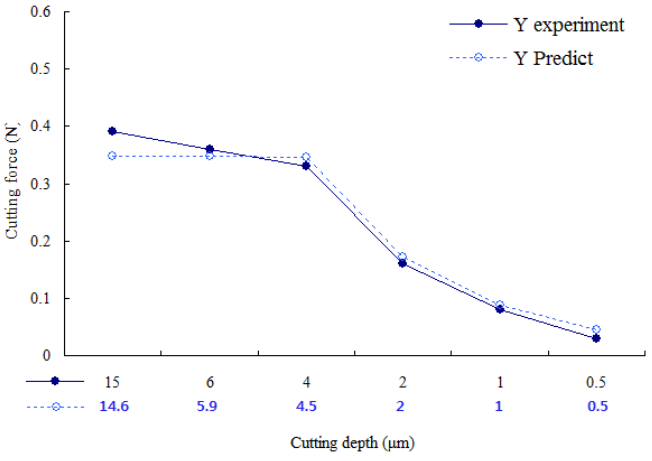

(b)

Fig. 6 (a) Flow charts of optimization algorithm (b) Cutting depth for uniform cutting force reduces cycle time

The optimized cutting depths are applied to cut the same pattern and the cutting force is measured to compare predicted value. The maximum difference between experimented and predicted cutting force is 0.03 N as shown in Fig. 6(b). The difference between the measured value and the predicted values of the proposed algorithm is due to the optimized cutting depth being rounded to the value of experimented cutting depth.

Applying the new algorithm leads to the possibility of reducing the five cutting steps to three cutting steps, while maintaining a uniform cutting force below the maximum permissible value obtained from the previous experiments. This means that the roughing time will be reduced by 40% without increasing the cutting force compared to the conventional grooving conditions using a constant cutting depth.

5. Conclusions

In this research, the cutting force prediction model of micro pattern grooving was studied, the micro pattern cutting simulation software was developed, and the new cutting depths algorithm used to optimize the time factor was proposed. This technique reduces cycle time at the roughing stage effectively.

The research proposed a cutting force prediction model based on the micro cutting mechanism and the experimental data. The maximum error between the predicted cutting force and experimental data was 0.04 N for the prism pattern and 0.12 N for the rectangular pattern, which means the model agrees with the real data.

The geometrical micro pattern cutting simulation software was also developed for the automatic computation of the cutting section before real machining, which is used to compute cutting force and suggest the optimum cutting condition. The simulator covers prism, rectangular, pyramid, pillar, half circle prisms, various angle prisms and random patterns.

The model and simulation are used to suggest cutting depths that will optimize the time factor in the roughing stage. The number of cutting steps for the prism pattern was reduced from 5 to 3 by applying this technique. The result means that the new cutting depth algorithm will be able to reduce the roughing time by about 40% without increasing the maximum cutting force compared to the conventional roughing method with uniform depth.

ACKNOWLEDGEMENT

This research was supported by the Ministry of Knowledge Economy of South Korea.

REFERENCES

1. Hong, S. M., Je, T. J., Lee, D. J. and Lee, J. C., "Micro machining characteristics of V-shaped single crystal diamond tool with ductile workpiece," Journal of the Korean Society of Manufacturing Process Engineers, Vol. 4, No. 4, pp. 28-33, 2005.
2. Arcona, C. and Dow, T. A., "An empirical tool force model for precision machining," Journal of Manufacturing Science and Engineering, Transaction of the ASME, Vol. 120, No. 4, pp. 700-707, 1998.
3. Cheng, P. J., Tsay, J. T. and Lin, S. C., "A Study on instantaneous cutting force coefficients in face milling," International Journal of Machine Tools & Manufacture, Vol. 37, No. 10, pp. 1393-1408, 1997.
4. Yoon, Y. S. and Lee, S. J., "Cutting force prediction in single point diamond turning," Transactions of the KSME A, Vol. 17, No. 6, pp. 1456-1464, 1992.
5. Chae, J., Park, S. S. and Freiheit, T., "Investigation of micro-cutting operation," International Journal of Machine Tools & Manufacture, Vol. 46, No. 3-4, pp. 313-332, 2006.
6. Lai, X., Li, H., Li, C. F., Lin, Z. Q. and Ni, J., "Modeling and analysis of micro scale milling considering size effect, micro cutter edge radius and minimum chip thickness," International Journal of Machine Tools & Manufacture, Vol. 48, No. 1, pp. 1-14, 2008.
7. Ng, C. K., Melkote, S. N., Rahman, M. and Kumar, A. S., "Experimental study of micro- and nano-scale cutting of aluminum 7075-T6," International Journal of Machine Tools & Manufacture, Vol. 46, No. 9, pp. 929-936, 2006.
8. Kim, J. D. and Kim, D. S., "Theoretical analysis of micro-cutting characteristics in ultra-precision machining," Journal of material Processing Technology, Vol. 49, No. 3, pp. 387-398, 1995.
9. Wu, H. Y., Lee, W. B., Cheung, C. F., To, S. and Chen, Y. P., "Computer simulation of single-point diamond turning using finite element method," Journal of Materials Processing Technology, Vol. 167, No. 2-3, pp. 549-554, 2005.
10. Strenkowski, J. S., Shih, A. J. and Lin, J. C., "An analytical finite element model for predicting three-dimensional tool forces and chip flow," International Journal of Machine Tools & Manufacture, Vol. 42, No. 6, pp. 723-731, 2002.
11. Maekwa, K. and Itoh, A., "Friction and tool wear in nano-scale machining-a molecular dynamics approach," Wear, Vol. 188, No. 1-2, pp. 115-122, 1995.
12. Aly, M. F., Ng, E., Veldhuis, S. C. and Elbestawi, M. A., "Prediction of cutting forces in the micro-machining of silicon using a hybrid molecular dynamic-finite element analysis force model," International Journal of Machine Tools & Manufacture, Vol. 46, No. 14, pp. 1727-1739, 2006.
13. Lin, Z. C. and Huang, J. C., "The influence of different cutting

speeds on the cutting force and strain-stress behaviors of single crystal copper during nano-scale orthogonal cutting," Journal of Materials Processing Technology, Vol. 201, No. 1-3, pp. 477-428, 2008.